Global effects of the CSR-1 RNA interference pathway on transcriptional landscape

Germano Cecere[1], **Sebastian Hoersch**[2], **Sean O'Keeffe**[1], **Ravi Sachidanandam**[3], and **Alla Grishok**[1]

[1]Department of Biochemistry and Molecular Biophysics, Columbia University, New York, NY, USA

[2]David H. Koch Institute for Integrative Cancer Research, Massachusetts Institute of Technology, Cambridge, MA, USA

[3]Department of Oncological Sciences, Icahn School of Medicine at Mount Sinai, New York, NY, USA

Abstract

Argonaute proteins and their small RNA co-factors short interfering RNAs (siRNAs) are known to inhibit gene expression at the transcriptional and post-transcriptional levels. In *Caenorhabditis elegans*, the Argonaute CSR-1 binds thousands of endogenous siRNAs (endo-siRNAs) antisense to germline transcripts and associates with chromatin in a siRNA-dependent manner. However, its role in gene expression regulation remains controversial. Here, we used a genome-wide profiling of nascent RNA transcripts to demonstrate that the CSR-1 RNAi pathway promotes sense-oriented Pol II transcription. Moreover, a loss of CSR-1 function resulted in global increase in antisense transcription and ectopic transcription of silent chromatin domains, which led to reduced chromatin incorporation of centromere-specific histone H3. Based on these findings, we propose that the CSR-1 pathway has a role in maintaining the directionality of active transcription thereby propagating the distinction between transcriptionally active and silent genomic regions.

INTRODUCTION

RNA interference (RNAi) is largely known as a negative regulator of gene expression through different mechanisms. Those include inhibition of mRNA translation, mRNA or pre-mRNA degradation, and inhibition of transcription by promoting heterochromatin assembly (reviewed in refs. 1,2). Short interfering RNAs (siRNAs) bound by conserved Argonaute proteins, some of which have an endonucleolytic capacity, select the

complementary RNA targets regulated by RNAi (reviewed in ref. 3). However, neither RNA-RNA interaction nor Argonaute-mediated cleavage excludes the possibility that siRNAs may have a positive effect on gene expression. Here, we report that an RNAi pathway enhances transcription of genes targeted by endogenous siRNAs (endo-siRNAs) in *C. elegans* genome wide.

endo-siRNAs were initially discovered in *C. elegans*[4], and later in *Drosophila* and mammals (reviewed in ref. 5). They can be antisense to protein-coding transcripts or can be derived from pseudogenes, transposons and intergenic regions that produce double-stranded RNA (dsRNA) (reviewed in ref. 2). Most known cases of gene regulation by endo-siRNAs include inhibition of their targets at the post-transcriptional level (reviewed in refs. 5-7). However, association of nuclear Argonaute proteins with transcriptionally-active gene loci has also been described in metazoans, including human cells[8-12], (reviewed in ref. 13).

The network of endo-siRNA pathways in *C. elegans* is very extensive (reviewed in ref. 7). In the germline, endo-siRNAs that are produced by the activities of RNA-dependent RNA Polymerases (RdRPs) on target transcripts are termed 22G-RNAs. They belong to two major endo-RNAi pathways: 1) the worm-specific AGO (WAGO) pathway[14], which silences pseudogenes, transposons, cryptic loci, and some protein-coding genes, and 2) the CSR-1 pathway, which targets more than 4,000 highly active genes preferentially expressed in the germline[15,16]. Surprisingly, CSR-1-bound 22G-RNAs do not inhibit expression of their targets[15,16]. However, the Argonaute CSR-1 has been shown to associate with chromatin in a 22G-RNA-dependent manner[15], which suggests nuclear functions. Moreover, inactivation of the CSR-1 RNAi pathway components leads to sterility, abnormal P-granules, chromosome segregation defects, mislocalization of centromeric proteins, such as the variant histone CENP-A, and embryonic lethality[15-23]. Recently, the CSR-1 pathway has been shown to directly promote histone pre-mRNA processing[24] and to positively regulate expression of some spermiogenesis-related genes[25]. Therefore, the key unanswered question is whether CSR-1-bound 22G-RNAs globally regulate expression of CSR-1 target genes in the nucleus.

To determine the effect of the CSR-1 pathway on RNA Polymerase II (Pol II) transcription we utilized the Global Run-On sequencing (GRO-seq) method[26], which allows to map the position, amount and orientation of transcriptionally-engaged Pol II genome wide. We assayed transcription in a loss-of-function mutant of Dicer-related helicase, *drh-3*, which is depleted of most endo-siRNAs[14] and in a *csr-1* hypomorphic strain that has reduced expression of CSR-1[15]. Our genomic analyses demonstrate that the CSR-1 pathway promotes Pol II transcription of its active target genes in a siRNA-dependent manner genome wide. Moreover, a loss of CSR-1 activity results in a global increase in antisense transcription and ectopic expression of silent genes, which affects chromatin organization. Therefore, our results suggest that CSR-1 and its associated 22G-RNAs participate in a positive-feedback mechanism that stimulates and restricts sense-oriented Pol II transcription, thus propagating the distinction between "active" and "silenced" chromatin domains.

RESULTS

Reduced transcription of CSR-1 targets in endo-RNAi mutants

Several studies have shown that endo-siRNA abundance negatively correlates with the expression of their target genes in *Drosophila, C. elegans* and mouse (reviewed in refs. 5-7). CSR-1-associated endo-siRNAs are antisense to more than 4,000 protein-coding genes (CSR-1 targets) expressed in the germline. However, RNA profiling of *csr-1* mutant worms did not detect significant increases in steady-state RNA levels of CSR-1 target genes compared to wild type (WT)[15]. Moreover, a decrease in expression was observed in the *csr-1* mutant for a significant number of CSR-1 targets (Supplementary Fig. 1a). Importantly, we have recently shown that CSR-1 binds to histone mRNAs (a prominent group of CSR-1 targets) and promotes their biogenesis[24]. Given the fact that CSR-1 is present in the nuclear fraction and associates with chromatin at its target genes in a siRNA-dependent manner[15], we explored the possibility that CSR-1 can globally regulate its target genes at the transcriptional level. To study the relationship between CSR-1 22G-RNAs and Pol II transcription genome wide, we analyzed the distribution of transcriptionally-engaged Pol II in WT worms and mutants affecting the CSR-1 pathway by GRO-seq. Knowing that *csr-1* null mutations cause sterility[17], we utilized a previously described hypomorphic *csr-1(tm892)* mutant strain in which CSR-1 function was partially rescued by a transgenic CSR-1 protein expressed from the germline-specific promoter[15]. We confirmed that CSR-1 is present in the nuclear fraction and that the *csr-1* hypomorphic strain expresses CSR-1 protein isoforms at a lower level compared to WT (Supplementary Fig. 1c, d). We also used a loss-of-function mutant of Dicer-related helicase, *drh-3(ne4253)* (ref. 14), which is depleted of most 22G-RNAs that belong to the WAGO and CSR-1 pathways. Importantly, the levels of histone proteins and their incorporation into chromatin in these two loss-of-function mutant strains were similar to those in WT (Supplementary Fig. 1b, e). Therefore, the possible indirect effect of histone depletion on transcription, which may occur after prominent down-regulation of CSR-1 by RNAi[24], should not be prevalent in these homozygous viable strains used for GRO-seq. Also, we performed GRO-seq using late L3 and early L4 stage worms before the occurrence of germline defects at later stages that could compromise our transcriptional profiling.

To evaluate the global effect of the CSR-1 pathway on Pol II transcription, we divided the GRO-seq reads into groups corresponding to promoters, gene bodies and gene ends, as previously described[27]. We compared cumulative GRO-seq signals from CSR-1 targets and from all genes in *csr-1* hypomorph and *drh-3(ne4253)* versus WT, and, notably, we found a substantial global reduction of Pol II transcription at CSR-1 target genes in both mutants (Fig. 1a-c). The effects on transcription that we observed in the *drh-3* mutant were specific to the CSR-1 target genes, because transcription of the WAGO protein-coding target genes[14] was not globally affected (Supplementary Fig. 2a, b). These results indicate that CSR-1 specifically promotes transcription of its target genes in a 22G-RNA-dependent manner. To confirm our analyses of GRO-seq data with a different statistical and normalization approach, we calculated the differential gene expression in *csr-1* hypomorph and *drh-3(ne4253)* mutants compared to WT using the R package DESeq[28]. In agreement with the analysis using cumulative reads, we only found a significant enrichment of CSR-1

targets among the genes that are transcriptionally down-regulated in the mutants (Fig. 1d, e). Interestingly, we also found that the up-regulated genes were significantly depleted of CSR-1 targets (Fig. 1d, e). Therefore, we quantified the cumulative GRO-seq signals from all the non-target genes and found a global increase in Pol II transcription among the non-target genes in *csr-1* hypomorph and *drh-3(ne4253)* mutant compared to WT (Fig. 1a, b). Finally, we compared our data with the published microarray results generated on *csr-1(tm892)* mutant and WT adult worms[15] and found a significant overlap among genes misregulated in the mutant that were identified by the microarray and by the GRO-seq (Supplementary Fig. 2c, d). This indicates that the changes in nascent RNA levels that we detected in CSR-1 pathway mutants correlate with the changes in steady-state mRNA levels that were published earlier[15]. Collectively, these results demonstrate that the CSR-1 pathway has a profound impact on Pol II transcription genome wide.

Next, we investigated which step of Pol II transcription was regulated by CSR-1 22G-RNAs. The decrease in transcription observed in CSR-1 pathway mutants occurred along the entire length of the genes, including promoter regions (Fig. 2a, b and Supplementary Fig. 3a, b). Consistently, we detected decreased levels of Pol II at the promoters of CSR-1 target genes in *drh-3(ne4253)* compared to WT by Pol II ChIP-qPCR experiments with an antibody that recognizes the non-phosphorylated isoform of Pol II (Supplementary Fig. 3c). In addition, we found an interaction between Pol II and CSR-1 in co-immunoprecipitation experiments (Supplementary Fig. 2d). Importantly, we found that the interaction between Pol II and CSR-1 was dependent on RNA and not on DNA (Fig. 2c). This suggests that CSR-1 and its associated 22G-RNAs interact with Pol II through nascent RNA transcripts. To prove this, we analyzed nuclear RNA that immunoprecipitated with FLAG–CSR-1 expressed from a transgene that rescued sterility of *csr-1* null mutant[33]. Indeed, we found an enrichment of germline-specific nascent transcripts (CSR-1 targets) in FLAG–CSR-1 RNA-IP compared to control IP performed with non-transgenic worms (Fig. 2d). Treatment of nuclear extracts with DNase I did not affect the interaction between CSR-1 and nascent RNA (Fig. 2d). However, inhibition of *drh-3* by RNAi caused a substantial reduction in the amount of immunoprecipitated RNA (Fig. 2d). These results indicate that the interaction between CSR-1 and nascent transcripts is mediated by 22G-RNAs and not dependent on DNA.

In summary, our findings suggest that CSR-1 has a direct effect on the Pol II complex and promotes its association with CSR-1 target loci through interactions of 22G-RNAs with nascent transcripts.

Increased antisense transcription in CSR-1 pathway mutants

Given that the GRO-seq method can distinguish the orientation of Pol II transcripts, we analyzed changes in antisense transcription. Surprisingly, we detected a global increase in antisense Pol II transcription in both *csr-1* and *drh-3* mutants (Supplementary Fig. 4a, b). To confirm these results with a different normalization method, we calculated the numbers of genes with marked up-regulated or down-regulated antisense transcription in CSR-1 pathway mutants compared to WT using DESeq[28]. Indeed, we found that the majority of genes with substantial changes in antisense transcriptions were up-regulated in CSR-1 pathway mutants (Fig. 3a, b). Interestingly, the increase in antisense transcription was also

observed on CSR-1 target genes (Fig. 3c). Because CSR-1 primarily associates with 22G-RNAs antisense to mRNA transcripts[15] and we found that it interacted with nascent RNA Pol II transcripts (Fig. 2d), these results are consistent with the possibility that CSR-1-associated 22G-RNAs stabilize sense-oriented Pol II machinery through their interaction with nascent sense RNA. This, in turn, may reduce the frequency of Pol II initiation in the antisense orientation.

Functional analysis of gene expression changes

An interesting feature of our GRO-seq findings is the global increase in transcription of non-CSR-1-target genes in *csr-1* and *drh-3* mutants (Fig. 1a, b, d, e). To further explore the nature of this increased transcription, we performed functional analysis of GRO-seq data using categories of genes that have been previously defined by their expression profiles[29-32]. We found that genes that were highly expressed at the developmental stage used for our analysis (late L3 and early L4), including ubiquitous and germline-enriched genes, showed a significant global decrease in Pol II transcription in *csr-1* hypomorph compared to WT (Supplementary Fig. 5a). Conversely, genes that are low-expressed or not expected to be expressed at the studied developmental stage, including the serpentine gene family and spermatogenesis-related genes, showed a significant global increase in Pol II transcription (Supplementary Fig. 5a). This analysis suggests that the CSR-1 pathway differentially regulates highly expressed genes and low-expressed or silent genes. Indeed, when we analyzed cumulative GRO-seq signals from the top 20% most highly transcribed genes and the lowest 20% transcribed genes (defined by GRO-seq) we found that highly expressed genes showed a global depletion in Pol II transcription in the studied mutants, and that low-expressed or silent genes showed a global increase in transcription (Fig. 4a and Supplementary Fig. 5d). The changes in Pol II transcription in these categories of genes were correlated with the enrichment or depletion of CSR-1 targets (Supplementary Fig. 5b, c). Similar results were obtained in GRO-seq analyses when genes were divided based on quartile of expression (Fig. 4b and Supplementary Fig. 5e). Finally, we evaluated the distribution of Pol II transcription along the chromosomes. Strikingly, changes in Pol II transcription on each chromosome were in accordance with the chromosomal enrichment of CSR-1 targets (Fig. 4c, d). Collectively, these results are consistent with a model of genome-wide redistribution of Pol II from highly transcribed genes to low-transcribed or silenced genes in CSR-1 pathway mutants. Therefore, we propose that CSR-1 and its associated 22G-RNAs have a role in restricting the localization of Pol II to highly transcribed genes.

Ectopic transcription of silent chromatin domains

Two distinct histone marks characterize transcriptionally silent and active chromatin domains in the *C. elegans* germline: the trimethylation of lysine 27 (H3K27me3) and lysine 36 (H3K36me3), respectively; these mutually exclusive domains are epigenetically propagated in the embryo[31,33,34]. Consistent with these results, we found that the genome-wide distribution of Pol II transcription in larvae, as defined by GRO-seq, positively correlated with the presence of H3K36me3 and negatively correlated with the presence of H3K27me3 (Fig. 5a, c). The centromeric histone H3 variant CENP-A is incorporated at regions devoid of transcription and co-localizes with H3K27me3 (ref. 35) (Fig. 5a-c). In contrast, GRO-seq signals were enriched at genomic regions that produce CSR-1-associated

22G-RNAs (Fig. 5b). Therefore, there is an inverse correlation between CENP-A domains and transcriptionally active 22G-RNA-producing regions, which was noted earlier[35]. Given the fact that normally silent genes were ectopically transcribed in CSR-1 pathway mutants (Fig. 4a, b and Supplementary Fig. 5a, d, e), we analyzed cumulative GRO-seq reads from CENP-A-enriched domains and H3K27me3-enriched genes and indeed detected an increase in transcription in *csr-1* hypomorphic mutant compared to WT (Fig. 5d-f). These results are consistent with a loss of robust distinction between transcriptionally active and silent genomic regions in the studied mutants.

Altered CENP-A incorporation into chromatin

Mutants of the CSR-1 pathway show chromatin organization defects, including mislocalization of centromeric proteins, such as CENP-A[15-17,19,23]. Depletion of canonical histone proteins upon strong down-regulation of CSR-1 by RNAi is predicted to have a significant impact on chromatin integrity[24]. However, we thought of the possibility that ectopic transcription seen in the *csr-1* and *drh-3* hypomorphic mutants may also affect chromatin organization, because CENP-A incorporation at the holocentric *C. elegans* chromosomes is inhibited at the genomic loci transcribed in the germline[35].

To test this hypothesis, we selected genomic regions that contain well-known active germline-specific CSR-1 target genes adjacent to silent non-target genes. We confirmed that in *csr-1* hypomorphic mutant these regions showed a decreased Pol II transcription of active germline-specific target genes and increased transcription of silent non-target genes (Supplementary Fig. 6). Notably, the increased ectopic transcription of silent regions was still low compared to the transcription of active germline-specific target genes (Supplementary Fig. 6); nonetheless, it may affect chromatin organization. In agreement with previous data[34,35], in WT embryos, we found that genes with low germline expression maintained higher levels of H3K27me3 and CENP-A compared to the adjacent active germline genes. Strikingly, this enrichment of H3K27me3 and CENP-A at non-germline genes was markedly reduced in CSR-1 pathway mutants (Fig. 6a-d). These findings are consistent with the prediction that ectopic transcription interferes with CENP-A deposition. Importantly, there was no increase in the levels of H3K27me3 and CENP-A on CSR-1 target genes in the mutant embryos (Fig. 4a-d). Moreover, no decrease in H3K36me3 levels and MES-4 binding at CSR-1 target genes was detected in mutant larvae (Supplementary Fig. 7). Thus, the reduced levels of H3K27me3 and CENP-A observed in CSR-1 pathway mutants were not the consequence of redistribution of H3H27me3, as observed upon reduction of *mes-4* expression[34]. In addition, these results also exclude the possibility that reduced transcription of CSR-1 target genes observed in *csr-1* and *drh-3* mutants was due to ectopic silencing or reduced activity of chromatin factors that promote transcription, such as MES-4.

The above results suggest that the global effect of the CSR-1 pathway on transcription is linked to the maintenance of distinct active and silent chromatin domains genome wide.

DISCUSSION

RNAi has been defined as a gene silencing mechanism. In metazoans, the discoveries of endo-siRNAs antisense to mRNA transcripts and transposons and their ability to repress

their target RNAs further supported the paradigm that endogenous RNAi-related pathways negatively regulate gene expression (reviewed in refs. 5-7,13). In *C. elegans*, one of the two major germline endo-siRNA pathways, the WAGO pathway, has been implicated in silencing of transposons, pseudogenes, cryptic loci and some protein-coding genes[14]. Recently, a connection between the PIWI-interacting RNA (piRNA) pathway and the WAGO pathway has also been described[36-40]. piRNAs can initiate the production of endo-siRNAs that are loaded onto some WAGO Argonaute proteins to silence the pre-mRNAs of their targets and to promote the methylation of lysine 9 on histone H3 (H3K9me), which is a chromatin mark associated with gene silencing[36,40].

The Argonaute CSR-1 is distinct among the many *C. elegans* Argonaute proteins in that it binds 22G-RNAs antisense to thousands of protein-coding genes[15], and the CSR-1 pathway has been associated with the most dramatic developmental phenotypes[15-23]. These findings suggest that CSR-1 is involved in gene expression regulation on a global scale. Since CSR-1 localizes to chromatin[15], we tested the possibility that it regulates gene expression at the transcriptional level. To investigate the transcriptional changes in mutants of the CSR-1 pathway we used the GRO-seq method, which allows the most sensitive quantitative view of the distribution of transcriptional-engaged Pol II in a genome-wide fashion[26]. Unexpectedly, we have discovered a global positive role of the CSR-1 pathway in transcriptional regulation in *C. elegans*. We found that CSR-1 associated with Pol II machinery to promote the high level of sense-oriented Pol II transcription on its target germline-expressed genes in a siRNA-dependent manner. Thus, it is likely that the multiple developmental abnormalities in CSR-1 pathway mutants may result from decreased transcription of germline genes.

Does CSR-1 play a direct role in promoting transcription?

Despite the lack of a clear mechanistic understanding of how CSR-1 regulates Pol II transcription, several lines of evidence support the idea that CSR-1 has a direct effect on its target genes. First, CSR-1 physically localizes to the target loci in the nucleus[15]. Second, we found that CSR-1 interacted with Pol II machinery and that this interaction was mediated by RNA. Third, we showed that CSR-1 interacted with nascent transcripts from the target loci in 22G-RNA dependent manner. Fourth, our GRO-seq analyses demonstrated down-regulation of Pol II transcription in CSR-1 pathway mutants specifically at genes targeted by antisense CSR-1-bound 22G-RNAs. Fifth, we observed similar transcriptional changes in *drh-3(ne4253)* and *csr-1* hypomorphic mutants, indicating that sequence-specificity of DRH-3-dependent 22G-RNAs must play a role. Moreover, a decrease in transcription observed in *drh-3(ne4253)* mutant occurred specifically at the CSR-1 target genes and not at other 22G-RNA targets, such as WAGO protein-coding target genes.

In addition, we can also exclude several possible indirect effects of CSR-1 on transcription. It is unlikely that a decrease in canonical histone levels led to transcriptional changes observed here. Our GRO-seq analyses were performed on homozygous viable partial loss-of-function mutant strains, which did not show histone depletion seen in *csr-1* RNAi-treated worms[24]. This allowed us to separate the indirect consequences of histone depletion from the apparent direct role of CSR-1 in transcription. Also, it is not likely that reduced transcription of CSR-1 target genes was due to ectopic silencing mediated by Polycomb

group proteins or by the piRNA–WAGO system since we have not detected an increase in H3K27me3 on CSR-1 target genes in CSR-1 pathway mutants and we have shown that the occupancy of MES-4 and H3K36me3 was not reduced under these conditions. Importantly, similar changes in transcription were observed in both *csr-1* and *drh-3* mutants, although DRH-3 helicase is also required for WAGO 22G-RNA production[14] and gene misregulation profile in *drh-3* mutant would have been distinct from that of *csr-1*, if WAGO-bound 22G-RNAs were causing ectopic silencing in the absence of CSR-1. Although we cannot exclude all possible indirect effects, based on the above arguments, it is most likely that CSR-1 and its 22G-RNA cofactors have a direct role in promoting expression of their target genes.

Indirect effects of CSR-1 pathway on transcription

Another important aspect of CSR-1-mediated transcriptional regulation, which has been revealed by our GRO-seq analyses, is the global increase in transcription at the genomic regions that do not include CSR-1 target genes. We have shown that those regions correspond to the silent part of the genome and that the increased Pol II transcription occurred in sense and antisense orientation. Because CSR-1 does not bind 22G-RNAs corresponding to those silent regions, it is unlikely that CSR-1 participates in controlling their transcription directly. One possibility is that CSR-1-bound antisense 22G-RNAs interact with nascent sense transcripts and directly reinforce sense-oriented Pol II complexes to prevent premature termination. Indeed, we found that CSR-1 associated with nascent transcripts in 22G-RNA-dependent manner and that RNA mediated the interaction between CSR-1 and Pol II machinery. Therefore, in the CSR-1 pathway mutants there may be an increased availability of Pol II to initiate non-specific transcriptional events all over the genome, including antisense transcription at CSR-1 targets themselves (Fig. 7).

In different systems, Argonaute proteins have been shown to participate in several other nuclear processes, including splicing[10,12] and three-dimensional genome organization[8,41]. Also, we have described the role of the CSR-1 pathway in histone pre-mRNA processing[24]. Here we found that transcription of histone genes, along with other CSR-1 targets, was reduced in *csr-1* and *drh-3* mutants. Therefore, there is another possibility for explaining our results: it is conceivable that CSR-1 globally affects pre-mRNA processing of its target genes, which is linked to transcriptional re-initiation. In this regard, RNA processing factors have been implicated in promoting gene loop formation on active genes[42], and there is evidence that gene looping reinforces transcription re-initiation and promotes the directionality of Pol II transcription by favoring sense over antisense transcription initiation[43,44].

In addition to histone mRNA processing, CSR-1 has also been implicated in translational regulation in the germline[45]. Also, an inhibitory effect of CSR-1-bound 22G-RNAs on some target mRNAs has been suggested[46]. Therefore, future investigation of direct and indirect inputs of CSR-1 on gene expression, possibly by multiple mechanisms, and their interconnections will be quite challenging, but it also promises to be very exciting.

Transcriptional regulation and chromatin organization

In addition to the challenge of understanding the mechanism by which CSR-1 regulates Pol II transcription, another important question is why an RNAi-based mechanism has evolved to potentiate transcription of active genes. In this study, we have accumulated evidence suggesting that the germline CSR-1 pathway is important for the propagation of the distinction between active and silent transcriptional domains in the progeny. In *S. pombe*, siRNAs generated from the peri-centromeric transcripts promote H3K9 methylation and heterochromatin formation in cis-, which facilitates centromere function (reviewed in ref. 1). Holocentric chromosomes in *C. elegans* incorporate centromeric proteins along the entire length of chromosomes. Moreover, CENP-A protein does not co-localize with H3K9 methylated regions, which are present on chromosomal arms[35,47]. Instead, CENP-A is incorporated on transcriptionally silenced chromatin domains enriched in H3K27me3, whereas CSR-1 22G-RNAs are produced from active chromatin domains that are depleted of CENP-A[35]. Therefore, there is an inverse correlation between CENP-A domains and CSR-1 22G-RNAs[35]. Here, we have shown that CSR-1 22G-RNAs generated from actively transcribed genomic regions promoted the maintenance of Pol II transcription from these target genomic loci in cis-. Moreover, we have demonstrated that decreased activity of CSR-1 led to increased transcription along the CENP-A-enriched domains, which was sufficient to reduce the incorporation of CENP-A in the embryos. Thus, we propose that the effect of CSR-1 on transcription is also important for proper CENP-A incorporation at the regions devoid of transcription (Fig. 7).

Interestingly, a recent study has shown that CSR-1 and two additional Argonaute proteins, ALG-3 and ALG-4, promoted expression of some spermatogenesis-specific CSR-1 target genes and suggested that heritable 22G-RNAs transmit gene-activating information from one generation to the next[25]. Also, CSR-1-bound 22G-RNAs are thought to promote expression of artificial transgenes in an epigenetic manner[48,49]. These observations are consistent with the global positive effect of CSR-1 on transcription revealed by our studies. It is possible that heritable CSR-1 22G-RNAs potentiate germline transcription genome wide, which then leads to definition of chromatin domains that are marked by distinct chromatin modifications and persist in the zygote and developing embryos.

Since the association of nuclear Argonautes with euchromatin has been shown in other animals, including human cells[8-12], and gene activation has been described upon targeting human Argonaute proteins to promoter regions using siRNAs[50-53], positive regulation of transcription by endogenous RNAi may be common in metazoans.

ONLINE METHODS

Strains

Strains were maintained at 20°C unless otherwise noted, using standard methods[54]. Bristol N2 was the wild type strain used. Strains used in this study were: *drh-3(ne4253), csr-1(tm892)*; neIs19[*pie-1*: :3xflag: :*csr-1, unc-119*(+)], LGII: neSi1[cb-*unc-119*(+) 3xflag: :*csr-1*]. For the GRO-seq experiments, synchronous populations of worms were grown for approximately 40 hr post-hatching at 20°C on OP-50 *E. coli* at a density of

~100,000 animals per 15 cm Petri dish. For early embryo preparations, worms were grown at 20°C on OP-50 *E. coli* at a density of ~40,000 animals per 15 cm Petri dish until gravid adults contained five embryos or fewer per worm, then embryos were extracted by hypochlorite treatment.

Cytoplasmic and nuclear fractionation

Nuclear and cytoplasmic extracts were prepared as follows: worms were washed off the plates with cold M9 and washed 3-4 times. The worm pellet was resuspended in 2ml of cold Nuclear Run-On (NRO) lysis buffer (10 mM Tris pH 7.5, 2 mM MgCl2, 3 mM CaCl2, 0.5% IGEPAL and 10% glycerol), transferred to a steel dounce (on ice) and stroked 30 times. The worm lysate was centrifuged for 2 min at $40 \times g$ and the supernatant was centrifuged again for 5 min at $1,000 \times g$ to pellet the nuclei. Next, the supernatant was stored as a cytoplasmic fraction and the nuclei pellet was washed three times with 1 ml of cold NRO lysis buffer and then resuspended in extraction buffer (50 mM Tris, 300 mM NaCl, 1 mM EDTA, 0.1% NP40, protease inhibitor cocktails (Fermentas)) and sonicated with 30 sec pulses 4 times using Branson microtip sonicator at 10% power in the cold room. The resulting material was used for western blotting and co-immunoprecipitation experiments or washed an additional time with 1ml of cold Freezing Buffer (50 mM Tris-Cl pH 8.3, 40% glycerol, 5 mM MgCl2, 0.1 mM EDTA) and then resuspended in 100 μl of Freezing Buffer and used for the GRO-seq experiments.

GRO-seq

GRO-seq experiments were performed as described in (ref. 27). Two biological replicates were generated for the *csr-1* hypomorphic mutant and the corresponding WT samples using ~300,000 worms for each experiment, and two biological replicates were prepared for the *drh-3(ne4253)* mutant and the corresponding WT samples using ~100,000 worms for each experiment.

Data Analysis

Two independent biological replicates of GRO-seq were generated using *csr-1* hypomorphic strain and the corresponding N2 wild type (WT) (called Mut_CSR-1 and WT_CSR-1, respectively); ~300,000 worms were used for each replicate. Since the *drh-3(ne4253)* mutant strain has a reduced number of progeny we included two biological replicates of *drh-3(ne4253)* using ~100,000 worms and compared them with two biological replicates of N2 (WT) generated using an equal number of worms (Mut_DRH-3 and WT_DRH-3, respectively). Sequencing was performed to a length of 50 nucleotides. Since cloned RNA ranged from 16 to 180 nucleotides in length, the sequencing reads were post-processed to eliminate the 3′ linker sequence, if present, so that resulting reads ranged from 16 to 50 nucleotides in length. The reads were then aligned using "bwa 0.6.1" to the *C. elegans* genome (ce6 assembly), and rRNA reads were removed based on genomic locations:

```
chrI    15060000   15072421   Ce_18S_rDNA   0   +
chrV    17115500   17132700   Ce_5S_rDNA    0   +
chrV    17428800   17429040   Ce_5S_rDNA-singleton   0   +
chrX    16929621   16940441   Ce_repetitiveLocus   0   +
```

After filtering, we obtained 44,155,515 reads from *csr-1* hypomorphic mutant [26,584,972 reads from the first replicate (called Mut_CSR-1_Rep1) and 17,570,543 reads from the second replicate (called Mut_CSR-1_Rep2)] and 36,133,711 reads from the corresponding WT [16,052,870 reads from the first replicate (called WT_CSR-1_Rep1) and 20,080,841 reads from the second replicate (called WT_CSR-1_Rep2)]. From *drh-3(ne4253)* mutant, we obtained after filtering 34,588,133 reads [17,492,181 reads from the first replicate (called Mut_DRH-3_Rep1) and 17,095,952 reads from the second replicate (called Mut_DRH-3_Rep2)], and 63,000,071 reads from the corresponding WT [21,660,645 reads from the first replicate (called WT_DRH-3_Rep1) and 41,339,426 reads from the second replicate (called WT_DRH-3_Rep2)]. We further filtered the data by strand (±) to analyze sense and antisense Pol II transcription. After ascertaining concordant results with the individual replicate pairs (WT vs. mutant), replicate reads for each WT and mutant were pooled, using downsampling on the replicate with higher read count to ensure equal representation of either replicate, and the pooled reads were processed together to increase statistical power.

For each annotated *C. elegans* transcript, the aligned reads were binned based on the annotated transcriptional start site (TSS) and transcriptional termination site (TTS) into 3 regions as follows: 'promoter' (from 600bp upstream of the annotated TSS to 200bp downstream), 'gene body' (from 200bp downstream of the annotated TSS to 200bp upstream of the annotated TTS), and 'gene end' (from 200bp upstream of the annotated TTS to 400bp downstream). We then calculated region-specific RPKM values (# of mapped reads per region / ([region length in KB] × [# of total mapped reads in million]). We also calculated statistically significant transcriptional changes in *csr-1* hypomorph and *drh-3(ne4253)* mutants versus WT using DESeq package[28] with a FDR of < 0.05.

For the enrichment or depletion of gene sets, we first calculated the number of genes expected by chance according to r = (n1 × n2)/N, with n1 = number genes in set 1, n2 = number of genes in set 2, N = total number of *C. elegans* genes considered, and then the enrichment was calculated by dividing the number of genes in common to the two datasets by r.

The average data profiles in Figure 5B were calculated using Cistrome–Galaxy[55] with the CEAS tool (SitePro: Aggregation plot tool for signal profiling (version 1.0.0)), and the heatmap showing the genome-wide correlation coefficient values in Figure 5C was calculated using Multiple wiggle files correlation tool (version 1.0.0).

The overlaps between gene lists were calculated using the online tool at http://www.nemates.org. Representation factors "r" to quantify the enrichment or depletion of gene sets were calculated according to r = (n1,2)/[(n1 × n2)/N], with n1,2 = number of genes common to set 1 and 2, n1 = number genes in set 1, n2 = number of genes in set 2, N = total number of genes considered.

Genes enriched in H3K27me3 were calculated using H3K27me3 ChIP-chip data sets generated with early WT embryos in ref. 34. We determined the number of genes enriched in H3K27me3 as described ref. 34.

The genomic coordinates of CENP–A enriched domains were taken from CENP–A ChIP–chip data set described in ref. 35 and available at http://www.modencode.org/. MES-4-enriched domains were taken from MES-4–FLAG ChIP-chip available at http://www.modencode.org/ The data sets of endo-siRNA cloned from CSR-1 IP complexes and from *csr-1(tm892)* and *ego-1(om97)* mutants that were used for our analyses are from ref. 15.

The genes sets identified in this study and published gene sets used for comparisons are listed in Supplementary Tables 1 and 2.

Western blotting

The protein concentration in nuclear and cytoplasmic extracts was quantified by the Bradford assay and equal amounts of proteins were then resolved on precast NuPAGE Novex 4-12% Bis-Tris gels (Invitrogen) for 1h at 4°C and transferred to a nylon membrane via semidry transfer (BioRad) at a constant current of 0.12 A for 1h. The antibodies used are as follows: anti-Pol II 8WG16 (Covance, MMS-126R, 1:1,000 dilution), anti-CSR-1 (a gift from J. Claycomb and the Mello lab, validated in ref. 15, 1:2,000 dilution), anti-H2B (Abcam, ab1790, 1:2,000 dilution), anti-actin (Millipore, MAB1501R, 1:2,000 dilution), anti-H2A (Abcam, ab13923, 1:2,000 dilution), anti-rabbit IgG HRP-labeled (PerkinElmer, NEF812001EA, 1:10,000 dilution), anti-mouse IgG HRP-labeled (PerkinElmer, NEF822001EA, 1:10,000 dilution). Validation information for the commercial antibodies is included at the manufacturers' websites. Original images of blots used in this study can be found in Supplementary Figure 8.

Co-immunoprecipitation

C. elegans nuclear protein extracts from L4 staged worms were used for immunoprecipitation with specific antibodies as described in ref. 27, followed by western blotting analysis. The antibodies used are as follows: 10 μg of anti-Pol II 8WG16 (Covance, MMS-126R), 10 μg of anti-CSR-1 (a gift from J. Claycomb and the Mello lab).

Chromatin Immunoprecipitation

Chromatin Immunoprecipitation (ChIP) experiments were performed as described in ref. 27 using early embryos or L4 worms. The antibodies used are as follows: 5 μg of anti-H3 (Millipore, 05-928), 2.5 μg of anti-H3K27me3 (Diagenode, pAb-195-050), 10 μg of anti-H3K36me3 (Abcam, ab9050), 10 μg of anti-MES-4 (Novus, 29400002), 10 μg of anti-CeCENP-A (a gift from the Desai lab, validated in ref. 35), 10 μg of anti-Pol II 8WG16 (Covance, MMS-126R). Validation information for the commercial antibodies is included at the manufacturers' websites.

RNA Chromatin Immuniprecipitation (RNA-ChIP)

C. elegans nuclear extracts from L4 staged worms, previously fixed with 2% paraformaldehyde, were used for immunoprecipitation using 30 μl of anti-FLAG M2 affinity gel (Sigma, A2220). Chromatin Immunoprecipitations were performed as described in ref. 27 except that the protein-RNA complexes were eluted from the beads using FLAG peptide (Sigma, F4799) and treated with 20 μg of proteinase K at 45°C for 1 h and then de-

crosslinked at 65°C for 1h. The RNA was isolated using TRI Reagent (Ambion, AM9738) according to the manufacturer's instructions. After treatment with TURBO™ DNase (Ambion, AM2238) the RNA was subjected to RT-qPCR using primers to detect pre-mRNAs. The sequence of primers is available upon request. Where indicated, the DNase treatment of the chromatin extract has been performed at 25°C for 30min using 20 U of TURBO™ DNase (Ambion, AM2238).

Supplementary Material

Refer to Web version on PubMed Central for supplementary material.

Acknowledgments

References

1. Grewal SI. RNAi-dependent formation of heterochromatin and its diverse functions. Curr Opin Genet Dev. 2010; 20:134–41. [PubMed: 20207534]

2. Kim VN, Han J, Siomi MC. Biogenesis of small RNAs in animals. Nat Rev Mol Cell Biol. 2009; 10:126–39. [PubMed: 19165215]

3. Hammond SM. Dicing and slicing: the core machinery of the RNA interference pathway. FEBS Lett. 2005; 579:5822–9. [PubMed: 16214139]

4. Ambros V, Lee RC, Lavanway A, Williams PT, Jewell D. MicroRNAs and other tiny endogenous RNAs in C. elegans. Curr Biol. 2003; 13:807–18. [PubMed: 12747828]

5. Okamura K, Lai EC. Endogenous small interfering RNAs in animals. Nat Rev Mol Cell Biol. 2008; 9:673–8. [PubMed: 18719707]

6. Lau NC. Small RNAs in the animal gonad: guarding genomes and guiding development. Int J Biochem Cell Biol. 2010; 42:1334–47. [PubMed: 20227517]

7. Grishok A. Biology and Mechanisms of Short RNAs in Caenorhabditis elegans. Adv Genet. 2013; 83:1–69. [PubMed: 23890211]

8. Moshkovich N, et al. RNAi-independent role for Argonaute2 in CTCF/CP190 chromatin insulator function. Genes Dev. 2011; 25:1686–701. [PubMed: 21852534]

9. Cernilogar FM, et al. Chromatin-associated RNA interference components contribute to transcriptional regulation in Drosophila. Nature. 2011; 480:391–5. [PubMed: 22056986]

10. Taliaferro JM, et al. Two new and distinct roles for Drosophila Argonaute-2 in the nucleus: alternative pre-mRNA splicing and transcriptional repression. Genes Dev. 2013; 27:378–89. [PubMed: 23392611]

11. Huang V, et al. Ago1 Interacts with RNA polymerase II and binds to the promoters of actively transcribed genes in human cancer cells. PLoS Genet. 2013; 9:e1003821. [PubMed: 24086155]

12. Ameyar-Zazoua M, et al. Argonaute proteins couple chromatin silencing to alternative splicing. Nat Struct Mol Biol. 2012; 19:998–1004. [PubMed: 22961379]

13. Cecere G, Grishok AA. Nuclear Perspective on RNAi Pathways in Metazoans. Biochim Biophys Acta. 2013

14. Gu W, et al. Distinct argonaute-mediated 22G-RNA pathways direct genome surveillance in the C. elegans germline. Mol Cell. 2009; 36:231–44. [PubMed: 19800275]

15. Claycomb JM, et al. The Argonaute CSR-1 and its 22G-RNA cofactors are required for holocentric chromosome segregation. Cell. 2009; 139:123–34. [PubMed: 19804758]

16. van Wolfswinkel JC, et al. CDE-1 affects chromosome segregation through uridylation of CSR-1-bound siRNAs. Cell. 2009; 139:135–48. [PubMed: 19804759]

17. Yigit E, et al. Analysis of the C. elegans Argonaute family reveals that distinct Argonautes act sequentially during RNAi. Cell. 2006; 127:747–57. [PubMed: 17110334]

18. She X, Xu X, Fedotov A, Kelly WG, Maine EM. Regulation of heterochromatin assembly on unpaired chromosomes during Caenorhabditis elegans meiosis by components of a small RNA-mediated pathway. PLoS Genet. 2009; 5:e1000624. [PubMed: 19714217]

19. Duchaine TF, et al. Functional proteomics reveals the biochemical niche of C. elegans DCR-1 in multiple small-RNA-mediated pathways. Cell. 2006; 124:343–54. [PubMed: 16439208]

20. Maine EM, et al. EGO-1, a putative RNA-dependent RNA polymerase, is required for heterochromatin assembly on unpaired dna during C. elegans meiosis. Curr Biol. 2005; 15:1972–8. [PubMed: 16271877]

21. Vought VE, Ohmachi M, Lee MH, Maine EM. EGO-1, a putative RNA-directed RNA polymerase, promotes germline proliferation in parallel with GLP-1/notch signaling and regulates the spatial organization of nuclear pore complexes and germline P granules in Caenorhabditis elegans. Genetics. 2005; 170:1121–32. [PubMed: 15911573]

22. Updike DL, Strome S. A genomewide RNAi screen for genes that affect the stability, distribution and function of P granules in Caenorhabditis elegans. Genetics. 2009; 183:1397–419. [PubMed: 19805813]

23. Nakamura M, et al. Dicer-related drh-3 gene functions in germ-line development by maintenance of chromosomal integrity in Caenorhabditis elegans. Genes Cells. 2007; 12:997–1010. [PubMed: 17825044]

24. Avgousti DC, Palani S, Sherman Y, Grishok A. CSR-1 RNAi pathway positively regulates histone expression in C. elegans. EMBO J. 2012; 31:3821–32. [PubMed: 22863779]

25. Conine CC, et al. Argonautes Promote Male Fertility and Provide a Paternal Memory of Germline Gene Expression in C. elegans. Cell. 2013; 155:1532–44. [PubMed: 24360276]

26. Core LJ, Waterfall JJ, Lis JT. Nascent RNA sequencing reveals widespread pausing and divergent initiation at human promoters. Science. 2008; 322:1845–8. [PubMed: 19056941]

27. Cecere G, Hoersch S, Jensen MB, Dixit S, Grishok A. The ZFP-1(AF10)/DOT-1 Complex Opposes H2B Ubiquitination to Reduce Pol II Transcription. Mol Cell. 2013; 50:894–907. [PubMed: 23806335]

28. Anders S, Huber W. Differential expression analysis for sequence count data. Genome Biol. 2010; 11:R106. [PubMed: 20979621]

29. Reinke V, et al. A global profile of germline gene expression in C. elegans. Mol Cell. 2000; 6:605–16. [PubMed: 11030340]

30. Wang X, et al. Identification of genes expressed in the hermaphrodite germ line of C. elegans using SAGE. BMC Genomics. 2009; 10:213. [PubMed: 19426519]

31. Rechtsteiner A, et al. The histone H3K36 methyltransferase MES-4 acts epigenetically to transmit the memory of germline gene expression to progeny. PLoS Genet. 2010; 6:e1001091. [PubMed: 20824077]

32. Kolasinska-Zwierz P, et al. Differential chromatin marking of introns and expressed exons by H3K36me3. Nat Genet. 2009; 41:376–81. [PubMed: 19182803]

33. Furuhashi H, et al. Trans-generational epigenetic regulation of C. elegans primordial germ cells. Epigenetics Chromatin. 2010; 3:15. [PubMed: 20704745]

34. Gaydos LJ, Rechtsteiner A, Egelhofer TA, Carroll CR, Strome S. Antagonism between MES-4 and Polycomb repressive complex 2 promotes appropriate gene expression in C. elegans germ cells. Cell Rep. 2012; 2:1169–77. [PubMed: 23103171]

35. Gassmann R, et al. An inverse relationship to germline transcription defines centromeric chromatin in C. elegans. Nature. 2012; 484:534–7. [PubMed: 22495302]

36. Lee HC, et al. C. elegans piRNAs mediate the genome-wide surveillance of germline transcripts. Cell. 2012; 150:78–87. [PubMed: 22738724]

37. Bagijn MP, et al. Function, targets, and evolution of Caenorhabditis elegans piRNAs. Science. 2012; 337:574–8. [PubMed: 22700655]

38. Shirayama M, et al. piRNAs initiate an epigenetic memory of nonself RNA in the C. elegans germline. Cell. 2012; 150:65–77. [PubMed: 22738726]

39. Ashe A, et al. piRNAs can trigger a multigenerational epigenetic memory in the germline of C. elegans. Cell. 2012; 150:88–99. [PubMed: 22738725]

40. Buckley BA, et al. A nuclear Argonaute promotes multigenerational epigenetic inheritance and germline immortality. Nature. 2012; 489:447–51. [PubMed: 22810588]

41. Lei EP, Corces VG. RNA interference machinery influences the nuclear organization of a chromatin insulator. Nat Genet. 2006; 38:936–41. [PubMed: 16862159]

42. Perkins KJ, Lusic M, Mitar I, Giacca M, Proudfoot NJ. Transcription-dependent gene looping of the HIV-1 provirus is dictated by recognition of pre-mRNA processing signals. Mol Cell. 2008; 29:56–68. [PubMed: 18206969]

43. Mapendano CK, Lykke-Andersen S, Kjems J, Bertrand E, Jensen TH. Crosstalk between mRNA 3' end processing and transcription initiation. Mol Cell. 2010; 40:410–22. [PubMed: 21070967]

44. Tan-Wong SM, et al. Gene loops enhance transcriptional directionality. Science. 2012; 338:671–5. [PubMed: 23019609]

45. Friend K, et al. A conserved PUF-Ago-eEF1A complex attenuates translation elongation. Nat Struct Mol Biol. 2012; 19:176–83. [PubMed: 22231398]

46. Maniar JM, Fire AZ. EGO-1, a C. elegans RdRP, modulates gene expression via production of mRNA-templated short antisense RNAs. Curr Biol. 2011; 21:449–59. [PubMed: 21396820]

47. Liu T, et al. Broad chromosomal domains of histone modification patterns in C. elegans. Genome Res. 2011; 21:227–36. [PubMed: 21177964]

48. Wedeles CJ, Wu MZ, Claycomb JM. Protection of Germline Gene Expression by the C. elegans Argonaute CSR-1. Dev Cell. 2013

49. Seth M, et al. The C. elegans CSR-1 Argonaute Pathway Counteracts Epigenetic Silencing to Promote Germline Gene Expression. Dev Cell. 2013

50. Li LC, et al. Small dsRNAs induce transcriptional activation in human cells. Proc Natl Acad Sci U S A. 2006; 103:17337–42. [PubMed: 17085592]

51. Schwartz JC, et al. Antisense transcripts are targets for activating small RNAs. Nat Struct Mol Biol. 2008; 15:842–8. [PubMed: 18604220]

52. Chu Y, Yue X, Younger ST, Janowski BA, Corey DR. Involvement of argonaute proteins in gene silencing and activation by RNAs complementary to a non-coding transcript at the progesterone receptor promoter. Nucleic Acids Res. 2010; 38:7736–48. [PubMed: 20675357]

53. Hu J, et al. Promoter-associated small double-stranded RNA interacts with heterogeneous nuclear ribonucleoprotein A2/B1 to induce transcriptional activation. Biochem J. 2012; 447:407–16. [PubMed: 23035981]

54. Brenner S. The genetics of Caenorhabditis elegans. Genetics. 1974; 77:71–94. [PubMed: 4366476]

55. Liu T, et al. Cistrome: an integrative platform for transcriptional regulation studies. Genome Biol. 2011; 12:R83. [PubMed: 21859476]
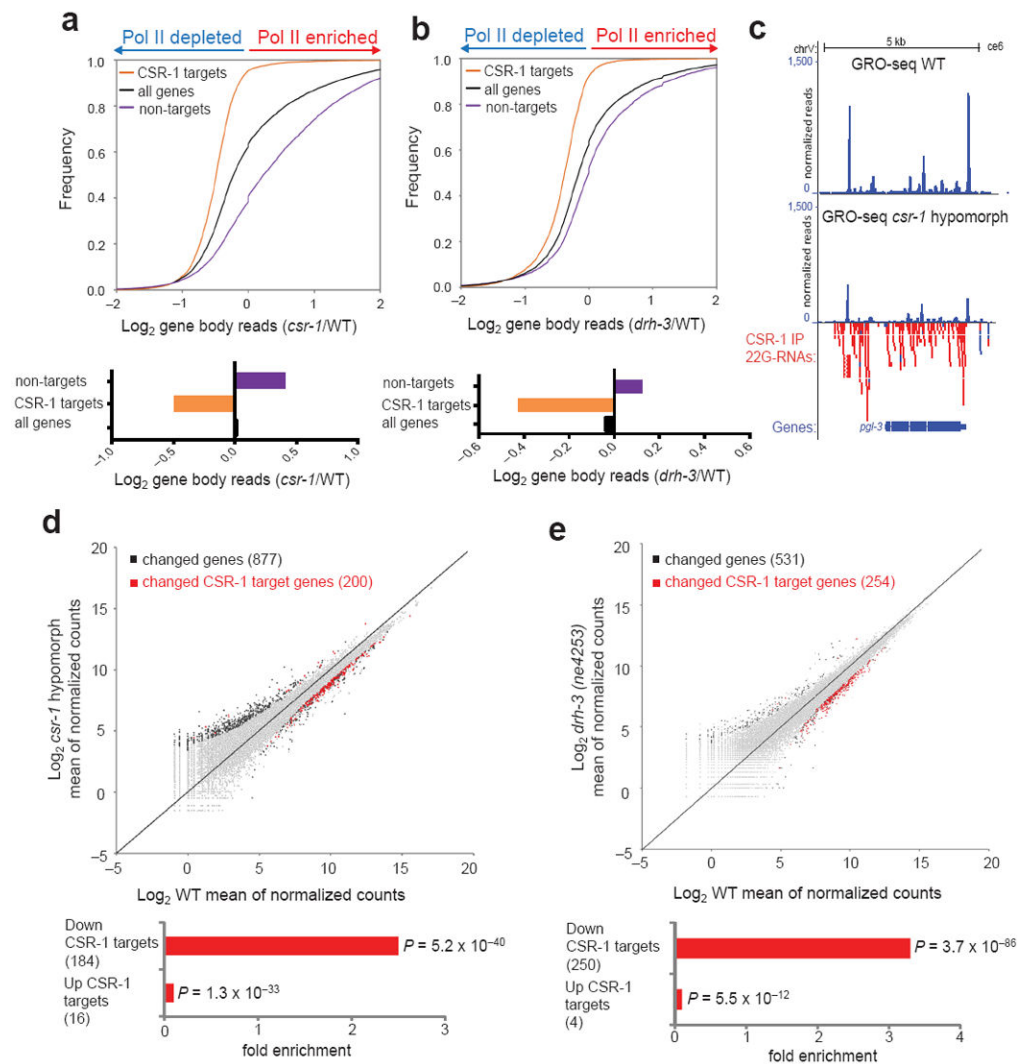
Figure 1. CSR-1 pathway positively regulates Pol II transcription

(a) Top, cumulative distribution plots of normalized GRO-seq gene body reads ($\log_2$ of the *csr-1*/WT read ratio): CSR-1 targets, as defined in ref. 15, (orange line), non-target genes (purple line) and total genes (black line). Bottom, the averages of the $\log_2$ ratio between *csr-1* hypomorphic mutant and WT normalized gene body reads. **(b)** GRO-seq analysis performed as in **a**, considering *drh-3(ne4253)* and WT normalized GRO-seq gene body reads. **(c)** An example of CSR-1 target gene, *pgl-3*. Track listing from top to bottom: normalized GRO-seq reads in WT larvae, normalized GRO-seq reads in *csr-1* hypomorphic mutant larvae, and CSR-1 22G-RNAs[15]. Gene models are based on UCSC Genome Browser (ce06). **(d)** Top, scatter plot of mean of normalized counts ($\log_2$) in *csr-1* hypomorphic mutant or WT calculated using DESeq package[28]. The black squares represent genes with significant changes in Pol II transcription considering a False Discovery Rate (FDR) of < 0.05. The red squares represent CSR-1 target genes with significant changes in Pol II transcription (FDR < 0.05). The number of significantly changed genes is shown in parentheses. Bottom, significant enrichment or depletion of CSR-1 targets among, respectively, genes up-regulated and down-regulated by GRO-seq in *csr-1* mutant versus

WT, *P* values for the significance of enrichment or depletion were calculated using Fisher's exact test. **(e)** Top, scatter plot, as in **d**, of mean of normalized counts (log$_2$) in *drh-3 (ne4352)* or WT. Bottom, significant enrichment or depletion of CSR-1 targets as in **d**.
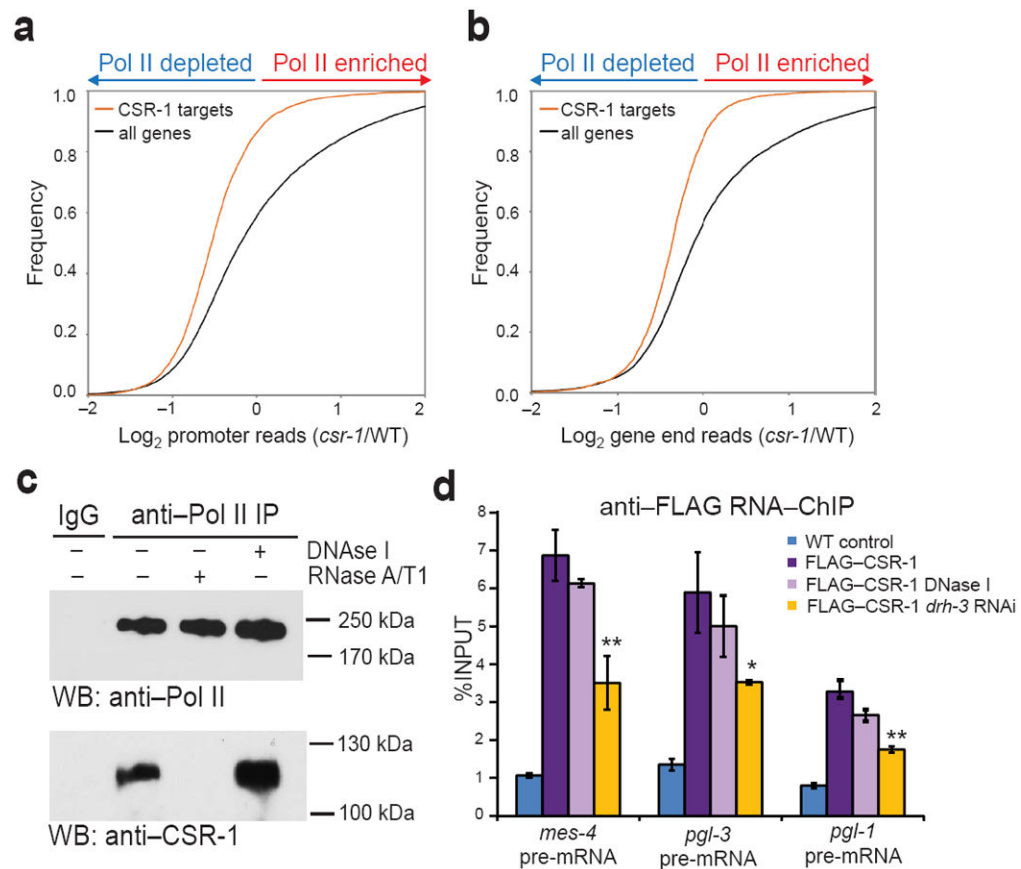
Figure 2. CSR-1 interacts with Pol II and nascent transcripts

(a, b) Cumulative distribution plots of normalized GRO-seq promoter reads (log$_2$ of the reads' ratios: *csr-1* hypomorph/WT or *drh-3(ne4253)*/WT): CSR-1 targets (orange line), and all genes (black line). (c) Co-immunopercipitation experiments with nuclear extracts treated or not with DNase I or RNase A/T1. The top panels show western blots with an antibody that recognizes the non-phosphorylated isoform of Pol II and the bottom panels show western blots with an antibody recognizing CSR-1. See Supplementary Fig. 8 for uncropped blot images. (d) RNA-ChIP-qPCR results obtained with an antibody against FLAG and nuclear extracts from non-transgenic worms (blue bars) or transgenic worms expressing FLAG–CSR-1 protein: without DNase I treatment (purple bars) or treated with DNase I (light purple bars). Yellow bars show results with FLAG–CSR-1 strain treated with RNAi against *drh-3*. Error bars, s.d. (*n* = 3 technical replicates). *$P < 0.05$; **$P < 0.01$ by one-tailed Student's *t* test in comparison to the transgenic strain expressing FLAG–CSR-1 protein.
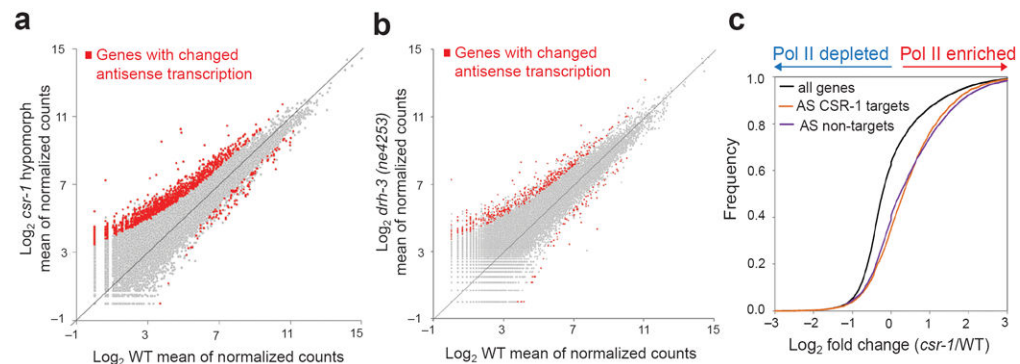
Figure 3. Increased antisense Pol II transcription in CSR-1 pathway mutants
(a, b) Scatter plots, as in Fig. 1d, e, of mean of normalized counts (log$_2$) calculated using DESeq package[28] and showing genes with statistically significant changes in antisense Pol II transcription in *csr-1* hypomorph or *drh-3(ne4253)* mutants versus WT, respectively, (FDR < 0.05). **(c)** Cumulative distribution plots of normalized GRO-seq reads showing CSR-1 targets (antisense (AS) reads, orange line) and non-targets (AS reads, purple line) compared to the sense reads of all genes (black line). Only reads from the gene body were considered for the analyses shown in **c**.
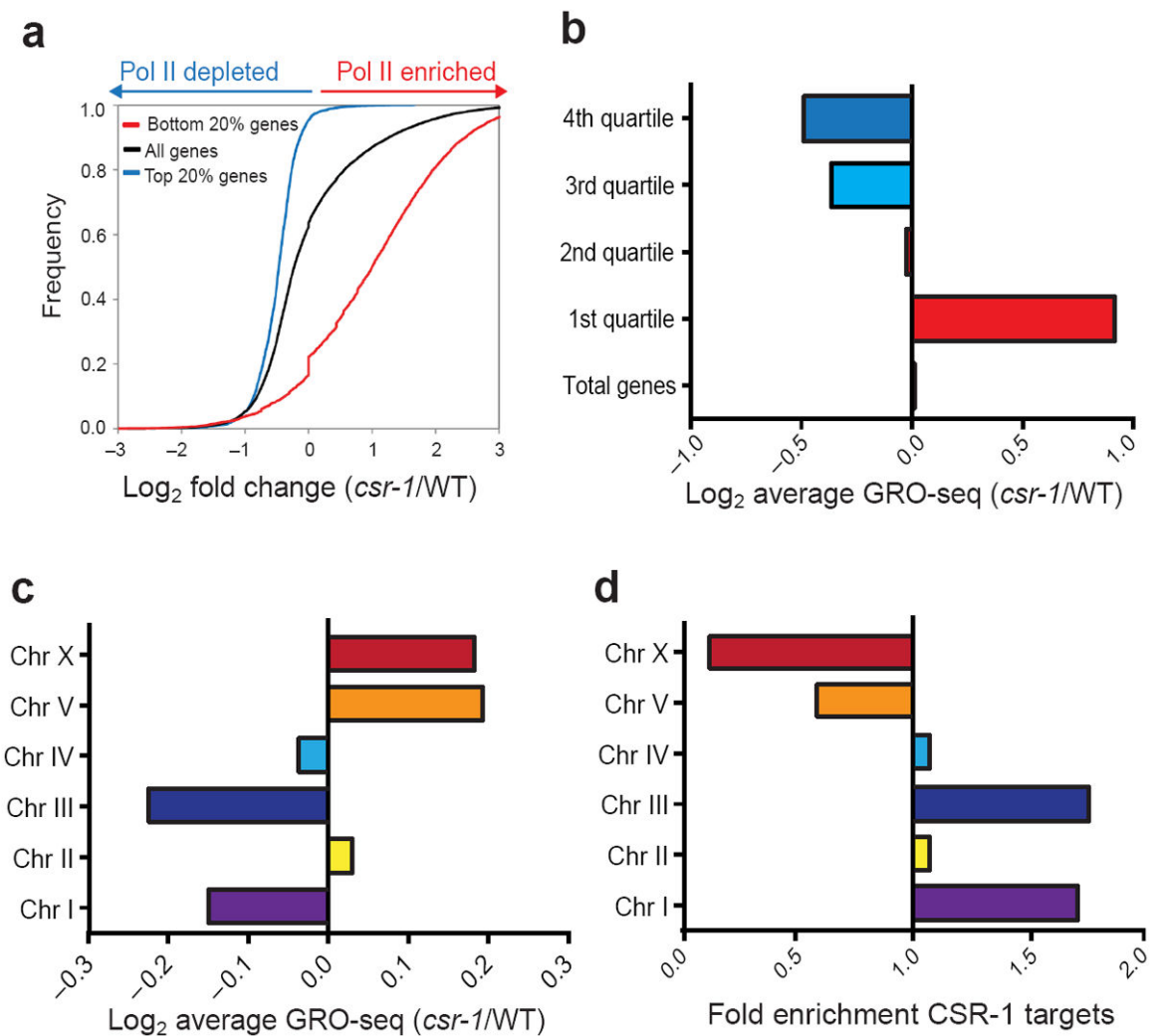
Figure 4. Categories and chromosomal distributions of genes affected by CSR-1 pathway mutants

(a) Cumulative distribution plots of normalized GRO-seq reads showing changes in transcription in *csr-1* hypomorph compared to WT: top 20% highly-transcribed genes (blue line), bottom 20% genes (red line) and all genes (black line). Only reads from the gene body were considered for this analysis. **(b)** The average of the $\log_2$ ratios between the *csr-1* hypomorphic mutant and WT normalized gene body reads quantified for genes grouped by quartiles of expression, based on GRO-seq. **(c)** The averages of the $\log_2$ ratios between the *csr-1* hypomorphic mutant and WT reads quantified for genes present on each autosome. **(d)** Enrichment or depletion of CSR-1 target genes among *C. elegans* chromosomes, see the formula used to calculate enrichment or depletion in online methods section.
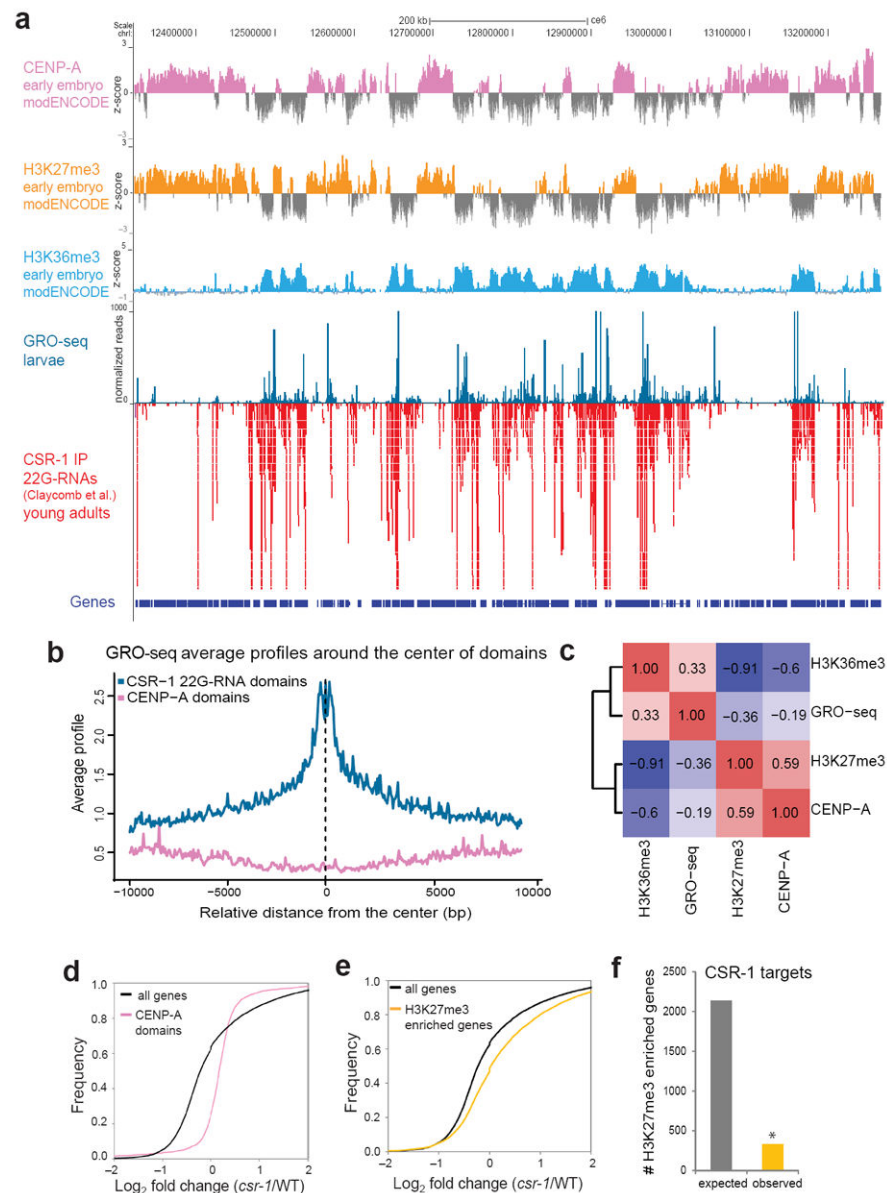
Figure 5. Relationship between silent and active chromatin domains in CSR-1 pathway mutants
(a) A map of a portion of chromosome I, track listing from top to bottom: ChIP-chip peaks for CENP-A, H3K27me3 and H3K36me3 (early embryo data from modENCODE), GRO-seq reads (this study) and CSR-1-bound endo-siRNA reads[15]. Gene models are based on UCSC Genome Browser (ce06). **(b)** Average GRO-seq profiles at CSR-1-associated endo-siRNA-enriched genomic domains (blue line) and at CENP-A-enriched domains (pink line). **(c)** A heatmap showing the genome-wide correlation coefficient values between GRO-seq reads and H3K36me3 ChIP-chip, CENP-A ChIP-chip and H3K27me3 ChIP-chip peaks (all ChIP-chip data are from modENCODE). Positive correlations are shown in red and negative correlations in blue. **(d)** Cumulative distribution plots of normalized GRO-seq reads showing changes in transcription in *csr-1* hypomorph compared to WT at CENP-A-enriched domains (red line) compared to all genes (black line). **(e)** Cumulative distribution plots, as in

d, at genes enriched in H3K27me3 (yellow line) compared to all genes (black line). **(f)** Expected (grey bar) and observed (orange bar) numbers of CSR-1 target genes among the genes enriched in H3K27me3. Asterisk indicates significance of less than expected by chance calculated using hypergeometric test, $P < 0.0001$.
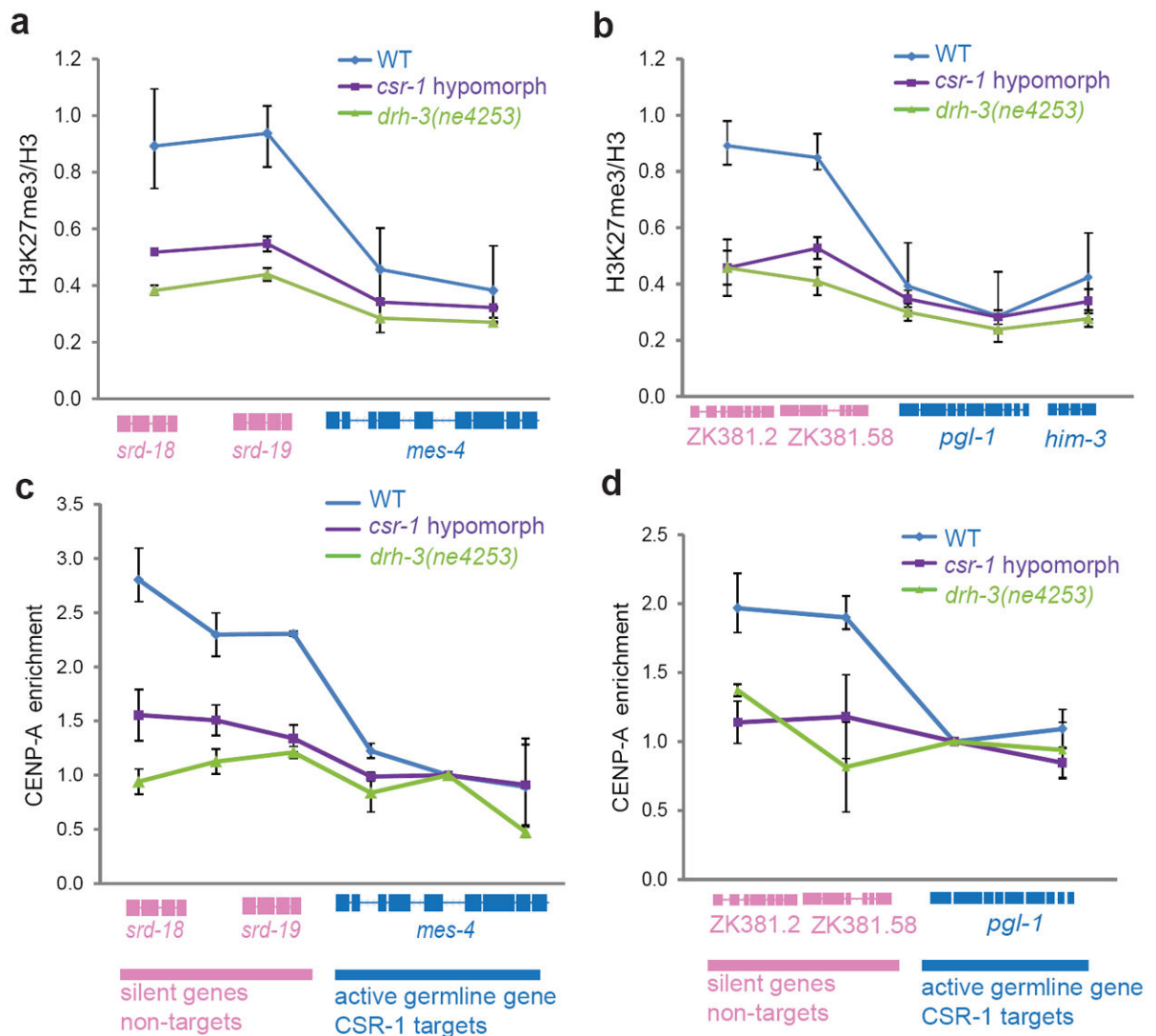
Figure 6. Decrease in H3K27me3 and CENP-A chromatin localization in CSR-1 pathway mutant embryos

(a, b) ChIP-qPCR results showing the levels of H3K27me3 normalized to the total levels of histone H3 at two genomic loci in WT, *csr-1* hypomorph and *drh-3(ne4253)* mutants. Genes colored in pink correspond to the non-target silent genes that increase in transcription in mutant larvae and genes colored in blue are active germline-specific CSR-1 target genes that decrease in transcription in CSR-1 pathway mutant larvae. Bars indicate ranges, ($n = 2$ biological replicates). Gene models are based on UCSC Genome Browser (ce06). **(c, d)** ChIP-qPCR as in **a, b**, showing the enrichment of CENP-A on chromatin in WT and *csr-1* hypomorph and *drh-3(ne4253)* mutants. The enrichment of CENP-A has been calculated relative to a region in the CSR-1 target genes for each locus considered (circles). Bars indicate ranges, ($n = 2$ biological replicates).
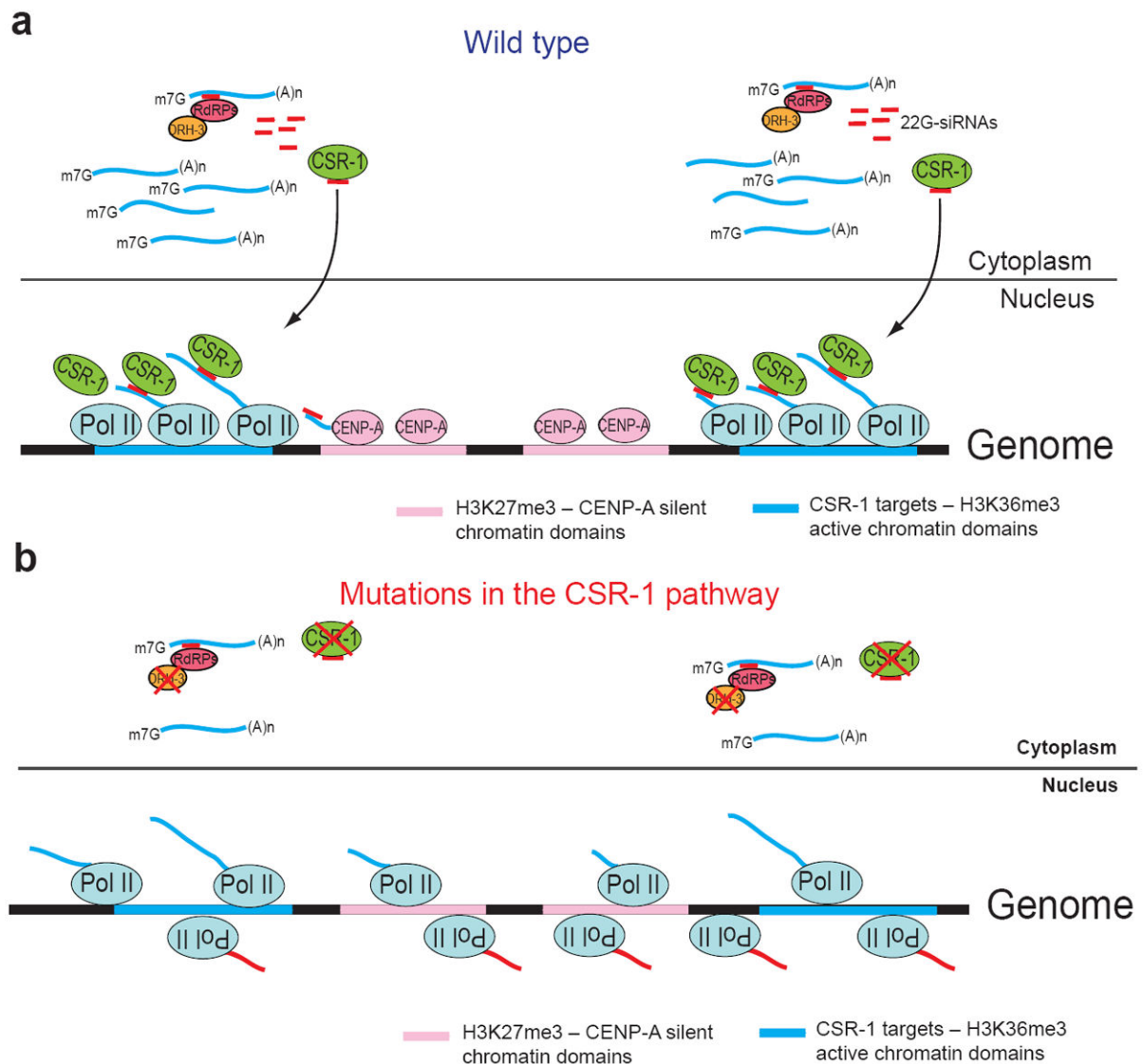
Figure 7. Model illustrating the proposed role of the CSR-1 pathway in regulation of Pol II transcription and chromatin organization

(a) Cytoplasmic mRNAs derived from actively transcribed regions are used as templates by RdRP complexes containing DRH-3 to produce antisense 22G-RNAs that are loaded onto CSR-1 Argonaute[15]. CSR-1 and its associated siRNAs translocate into the nucleus where they interact with complementary nascent RNA transcripts to promote and localize Pol II transcription on active genes and to inhibit sense and antisense transcription at the silent chromatin regions. This leads to the reinforcement of the distinction between active and silent chromatin domains. **(b)** Impaired function of the components of the CSR-1 pathway (such as CSR-1 or DRH-3) leads to the reduction in the levels of Pol II transcription on active genes and results in the ectopic sense and antisense transcription. Ectopic transcription at normally silent chromatin domains leads to reduced CENP-A incorporation and to the loss of robust differences between active and silent chromatin.